Impacts of Red-Light Cameras on Intersection Safety: A Bayesian Hierarchical Spatial Model

Soheil Sohrabi (Student)
Zachry Department of Civil Engineering, Texas A&M University
3136 TAMU, College Station, TX, 77843-3136
Tell: (515) 451-6116; Email: sohrabi.s@tamu.edu

Dominique Lord (Advisor)
Zachry Department of Civil Engineering, Texas A&M University
3136 TAMU, College Station, TX, 77843-3136
Phone: (979) 458-3949; Email: d-lord@tamu.edu

Submission Date: March 1st

Word Count= 2789 (body) + 3 Tables + 3 Figures

Contents

ABSTRACT

Enforcing red-light runners is known as an engineering solution to enhance intersection safety. However, the efficiency of automated Red-Light Camera (RLC) programs is always questioned mainly because of the inaccuracy in post-implementation reviews and difficulties with the financial viability of the program. In this paper, first, we propose a model to capture the effect of RLCs on intersection safety by including the spatial dependency between intersections crashes, unobserved heterogeneity, and the spillover effect of enforcing cameras. In this context, a Bayesian hierarchical spatial model is implemented to estimate crash frequency at intersections. Second, an optimization problem is proposed to seek the optimal allocation of RLC across intersections. The model was examined using the injury crashes collected from 150 intersections located in the City of Chicago. The results show that the probability of crashes decreases at intersections equipped with enforcing camera by 6%. Also, the spillover effect of cameras is examined in this study by capturing the safety impact of cameras on other adjacent intersections. It is shown that crash risk is reduced by 2% for an intersection located within 1 km network distance from the RLC. Using the estimated impacts of RLC intersection safety, the optimum location of the cameras across the Chicago intersection can reduce the number of injury crashes by 13%.

Keywords: Red-Light Camera, Bayesian Hierarchical Spatial Model, Spillover Effect, Optimal RLC Allocation

INTRODUCTION

Intersection safety is one of the most significant issues many cities face in managing traffic safety. It has been shown that red-light running (RLR) is an important contributing factor for crashes at signalized intersections [1]. According to the Insurance Institute of Highway Safety (IIHS), red-light runners encompass about 800 deaths and 137,000 injuries annually in the U.S. [2]. In a recent study, the intersection safety of 57 cities that have implemented an RLC program was compared to 33 cities that decided not to implement such a program [3]. The comparison showed that the ratio of RLR fatal crashes per capita to all intersection related fatal crashes improved by 21% after the RLC program implementation.

Despite the indisputable role of RLC on driver behavior, RLC programs have always been under scrutiny. One common argument against the program is that RLCs exacerbate the intersection safety by referring to the increase in the number of crashes in some cities or in a given intersection after RLCs are installed. An evaluation of RLC in seven cities revealed that right-angle crashes were reduced by 25% while the rear-end crashes increased by 15% [4]. Given that right-angle crashes are inherently high injury risk crashes comparing to rear-end collisions, the RLC program may still improve safety even if the total number of crashes increases. The crash occurrence is dependent on many factors including the service volume of the intersection, local land use developments, intersection geometry and control, users characteristics, etc., which needs to be considered before jumping into conclusion. This reveals the importance of engineering analysis of the RLC impact on traffic safety based on sufficient analyses of risk factors.

In addition, many RLC programs have been widely accused of being used to generate revenues for cities rather than being used for improving safety, given fining regulations. However, the number of communities using RLCs has been dramatically decreasing since 2012 (from 533 to 430 communities) because of the difficulties in sustaining the financial viability of the program [2]. Since the costs of the system are mainly attributed to the RLC operation costs, efficient system design can help to overcome the financial barriers associated with the RLC program. In this case, the RLC allocation problem arises. Typically, cameras are recommended to be installed at intersections with a higher number of red light running-related crashes or violations [2, 5], however, given the potential impacts of RLCs on the intersections in the vicinity, this approach may not lead to optimum RLC allocation.

In this study, first, we propose a methodological framework with the aims of capturing the effect of RLCs on injury crash frequency by: (1) taking into account the observable factors (e.g. land use, intersection geometry and service volume) and unobservable spatial factors (e.g. immeasurable land use, social activities, and special events) that affect the crash frequency, (2) considering the unobserved heterogeneity at an intersection such as variation in drivers' characteristics, and (3) investigating the spatial effect of the RLC on other intersections' safety. Second, we apply the proposed model results to optimize the RLC allocation in the system. We use data collected from the City of Chicago RLC program for evaluating the proposed model.

LITERATURE REVIEW

Review of literature finds RLR violation is an important issue in intersection safety [6-8], and enforcement by RLC is introduced as an effective way to reduce RLR violations [9-11]. The effectiveness of the RLC has mainly been investigated using before-after studies (e.g. [5, 12-14]). Also, statistical models have been used for examining the RLC effectiveness in the form of linear, logistic, and generalized linear models [6, 8, 9]. A set of variables are used in these studies to better capture the RLC impacts comprising the intersection control, geometry or functional characteristics. The red and yellow light durations and cycle length are features that can be used for reducing traffic violations [7, 15, 16]. The number of approaches at the intersection, speed limit, right/left turn restriction, and the number of lanes are the most significant

variables that have been used in previous studies to characterize the intersection geometry [5, 6]. Also, the positive association between the intersection traffic and RLR is examined in the form of volume-to-capacity ratio of the average daily traffic [5, 6, 9].

The unobservable factors are generally ignored in these models. The role of unobserved heterogeneity in crash frequency modeling context is underlined by Lord and Mannering, and Mannering and Bhat [17, 18]. Ignoring the unobserved heterogeneity can result in inefficient and inconsistent parameter estimates [18]. The spatial dependency and heterogeneity in crash prediction models have been addressed in several studies using random parameters, spatial conditional autoregressive (CAR), and spatial weighting techniques [19-22]. Spatial dependency can be driven from the unobserved similarity in interacted traffic flow as well as land-use and intersection characteristics [23]. The effect of RLC on intersections located within the vicinity of an RLC (i.e., spatial spillover effect) has initially been discussed by Retting et al. in 1999 and then further discussed by other researchers [24-27]. Ahmed and Abdel-Aty indicated that in addition to significant crash reduction at intersections equipped with an RLC, the other intersections' safety improved in lesser magnitude but still significantly [27].

This paper contributes to the literature by filling the gap in previous studies. In this regard, we propose using a Bayesian hierarchical spatial model capable of encountering the unobserved heterogeneity and the spatial dependency between intersections crashes. Also, the spillover effect of the RLC is captured in the form of a spatial weighted variable.

METHODOLOGY

The proposed Bayesian hierarchical spatial model consists of three levels [28]:

1) Data model: [data | process, parameters],
2) Process model: [process | parameters],
3) Parameter model: [parameters].

In the first level, the data model describes the distribution of the observed crashes (z) given the true process $\lambda(.)$. We assume crashes are independent conditional on $\lambda(.)$, which is a valid assumption in crash measurement context. In other words, independence in the data model implies that the measurements of crashes frequency at intersections are independent. The data $z = z(S)$ is observed at 150 points or observations (intersections), $S = \{s_1, s_2, \dots, s_{150}\}$. The data model then becomes $[z|\lambda(S)]$. For crashes data passion distribution is usually assumed:

$$z|\lambda \sim Poisson(\lambda) \quad (1)$$

The spatial dependence in crashes is modeled in the second level, the process model. The process model $\lambda(.)$ conditional on the process parameters is assumed Gaussian stochastic process (lognormal given the log-link) as:

$$\lambda(.)|\beta, \theta_c \sim GP(\mu, C) \quad (2)$$

where $log(\mu) = x(s)'\beta$, $x(s)$ and β are vectors of covariates and coefficients. θ_c is the parameter vector in respect to covariance function. C is covariance function such that $C(s_1, s_2) = Cov(\lambda(s_1), \lambda(s_2))$. The spatially correlated random effect captures by this covariance function. We define the process with a spatially isotropic random field. This assumption implies that the mean is constant over space ($\mu(s) = \mu(s+h) \equiv \mu$), and the covariance function is only function of distance: $Cov\big(y(s), y(s+h)\big) = C(s, s+h) = C(||h||)$. Hence, the covariance function takes the form:

$$C = \sigma^2 \rho(h) \quad (3)$$

where σ is the variance and $\rho(h)$ is the correlation function as a function of h. Two correlation

functions, Matérn and Exponential, are examined in this study. The Matérn and Exponential correlation function are specified as [28]:

Matérn: $$\rho(h) = \frac{2^{1-\nu}}{\Gamma(\upsilon)}\left(\frac{h}{\alpha}\right)^{\nu} K_{\nu}\left(\frac{h}{\alpha}\right), \qquad \alpha > 0,\ \nu > 0 \qquad (4)$$

Exponential: $$\rho(h) = exp(-\frac{h}{\alpha}), \qquad \alpha > 0 \qquad (5)$$

where α and ν are parameters of the covariance function and estimate along with σ which construct the parameter vector θ_c. These parameters control the strength and scale of the spatial autocorrelation. The K_{ν} is a modified Bessel function in second kind of order υ.

For parameter inference of hierarchical spatial model, we need to integrate the likelihood of data:

$$L(\beta, \theta) = [z|\beta, \theta] = \int [z, \lambda|\beta, \theta] d\lambda = \int [z|\lambda][\lambda|\beta, \theta] d\lambda \qquad (6)$$

Given the Poisson distribution of the count data model and the Gaussian process of the process model, the likelihood function turns into the equation (7):

$$L(\beta, \theta) = \int Poisson(z|\lambda) N(\lambda|\mu, C) d\lambda \qquad (7)$$

The maximum likelihood estimate (MLE) of $\beta\ and\ \theta$ are defined as the values that maximize the likelihood function $L(\beta, \theta)$, or the log-likelihood $\ell(\beta, \theta) = logL(\beta, \theta)$. Based on the Bayesian thinking, the parameter distribution consists of the prior distribution for β. So, the prior distribution is $[\beta]$. In this case, the posterior is given by:

$$[\beta, \theta|z] = \frac{[z|\beta, \theta]_{[\beta]}}{\int_{\theta} [z|\beta, \theta]_{[\beta]} d\theta} \propto [z|\beta, \theta][\beta] = L(\beta, \theta)[\beta] \qquad (8)$$

For this problem, the MLE is not available in a closed form and so is posterior. In this case, a numerical method, Markov Chain Monte Carlo (MCMC) simulation, is used for determining the posterior.

Three goodness-of-fit measures, Mean Absolute Deviance (MAD), Mean-squared Predictive Error (MSPE), and Deviance Information Criteria (DIC) were used for assessing the model (equations 9 to 11):

$$MAD = \frac{1}{n}\sum_{i=1}^{n} |z_{estimate} - z_{observed}| \qquad (9)$$

$$MSPE = \frac{1}{n}\sum_{i=1}^{n} (z_{estimate} - z_{observed})^2 \qquad (10)$$

$$DIC = \overline{D} + p_D = D(\theta) + 2p_D \qquad (11)$$

where n is number of samples, D is the average deviance, $D(\theta)$ is the deviance of the posterior, and p_D is the effective number of parameters of the hierarchical model.

ANALYSIS

The model was implemented using data collected as part of the City of Chicago RLC program. Chicago has one of the longest-running and largest RLC enforcement systems in the US and has been investigated by a few researchers [5, 29]. Data from the periods 2005-2007 (before RLC installation) and 2010-2012 (after RLC installation) are employed for modeling. The model is developed using injury crash frequency data of 150 intersections where 90 of them were equipped with cameras in 2010-2012.

Data

In this study, four sets of data are used including; (1) crash data (all injuries: fatal, incapacitated, non-incapacitated, and possible) in two time periods, 2005-2007 and 2010-2012, (2) Chicago land-use, (3) RLC spatial indicators, and (4) the intersections function, control, and geometry characteristics. 150

intersections in Chicago are studied, where the cameras were active for 90 of them. The studied intersections are shown in Figure 1.

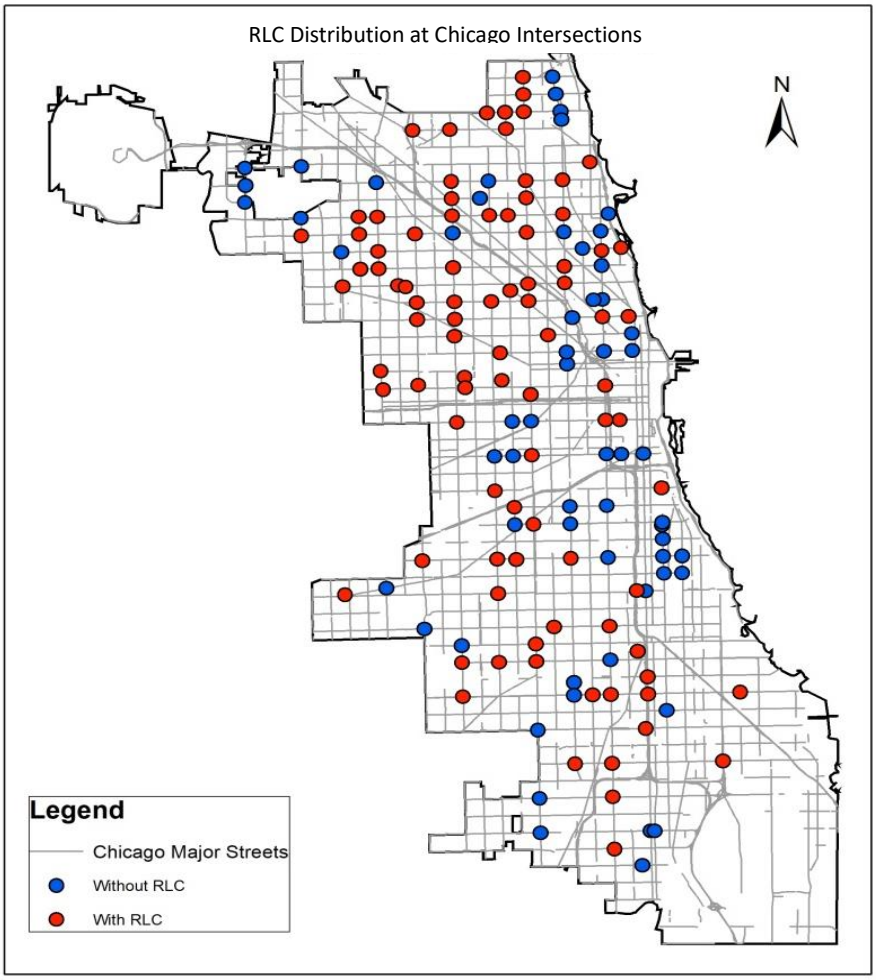

Figure 1. The RLC distribution across Chicago intersections in 2010.

Crash Data

The crash dataset consists of the aggregated annual injury crash frequencies that occurred at intersections before and after installation of RLCs, both at signalized intersections with (90 sites) and without (60 sites) a camera. The preliminary analysis of the crash data shows that the average annual number of crashes decreased by 12% after installing cameras. On the other hand, a (raw) 47% increase in rear-end crashes was observed after the RLC program (Table 1). Figure 2 shows the ratio of all types of crashes (all severities) over Annual Daily Traffic (ADT) at intersections. From the figure, the spatial dependency exists between intersection crashes.

Table 1. Number of Injury Crashes at studied Intersections Before and After the RLC Program

Intersection Type	Crash type (annual)	Number of Crashes		Change (percent)
		Before Installing Camera	After Installing Camera	
All studied intersections	Total Crashes	1777	1557	-12.4
	Total Crashes Excluding Rear-End	1496	1142	-23.7
	Rear-End Crashes	281	415	47.7
Studied intersections with camera	Total Crashes	1228	1063	-13.4
	Total Crashes Excluding Rear-End	1038	767	-26.1
	Rear-End Crashes	190	296	55.8

Land-Use

It is shown that the drivers take more risk while driving under the influence which can cause red-light running [30, 31]. We tested this hypothesis by examining the effect of land-use activities which serve alcohol on intersections crash frequency. To this extent, the major points of interests (POIs) in Chicago are collected using the Open Street Map POI dataset and corresponding variables are created in the form of the POIs density in 500, 700 and 1000 meters buffer around the intersection. The distribution of bars and restaurants is illustrated in Figure 2.

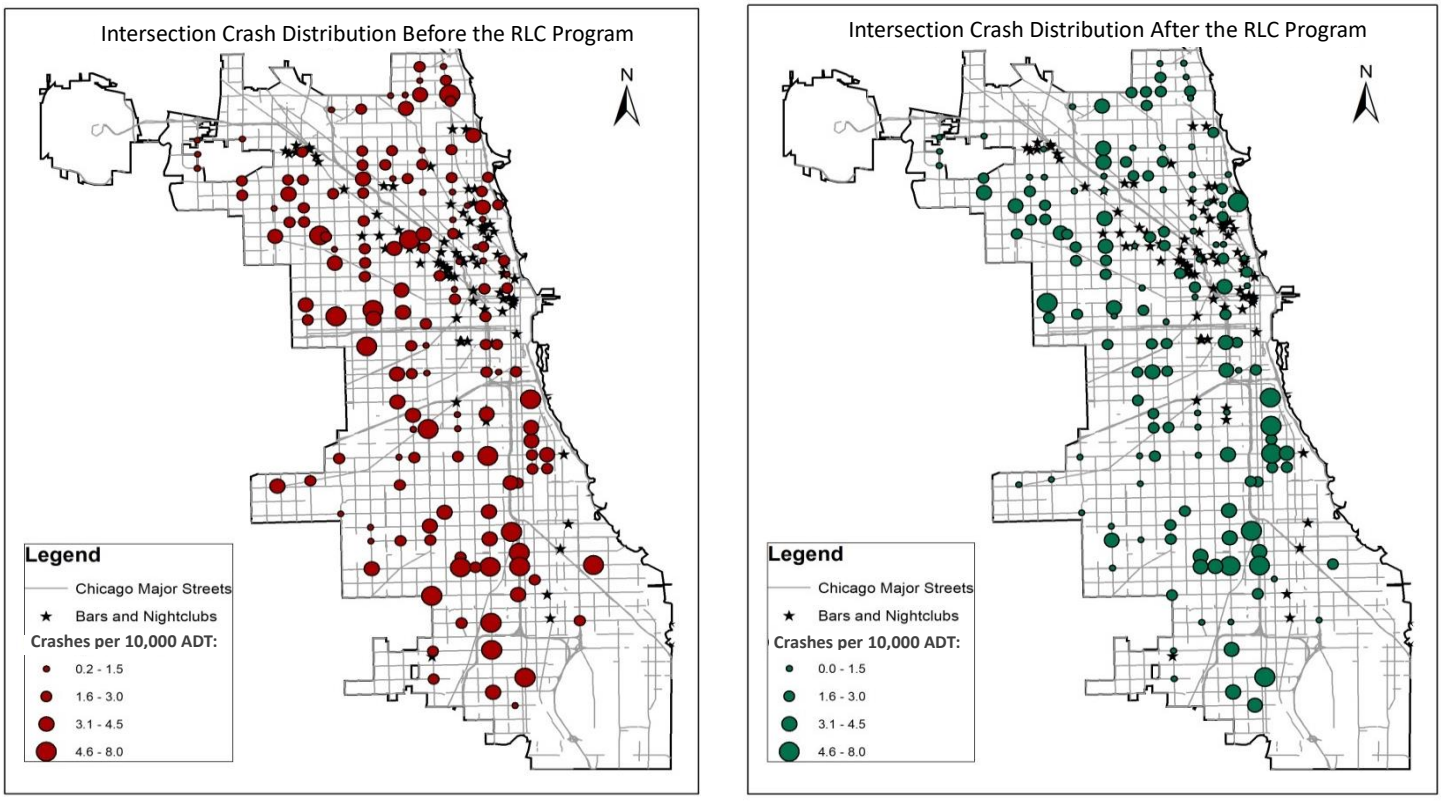

(a) **(b)**

Figure 2 Injury crashes per 10000 ADT distribution across Chicago intersections (a) before installing RLCs, and (b) after installing RLCs

RLC Distribution

To be able to examine the spillover effect of RLCs, spatial indicators were produced. The distance matrix of Chicago intersections was extracted from the Google API service. In addition to testing the linear spillover effect of RLCs, the presence of a camera at the intersection is spatially weighted in the form of the inverse spatial weighted and squared inverse spatial weighted.

Intersection Characteristics

While the intersection characteristic impacts on crashes are broadly illustrated in the literature, various variables were analyzed to measure this effect. The intersection function was defined in term of the annual traffic passing through the intersection and speed limit. The possibility of right turn on red (after stop) and the availability of left lanes in the intersection were evaluated. The number of lanes and the median type of intersections can be a helpful representative of the way intersection influence the drivers' behavior. Table 2 summarizes key variable statistics.

Table 2. Summary of intersections characteristics

Street Type	Variable	Statistic/ Condition	With RLC (90 sites)	Without RLC (60 sites)
Major	Average AADT [2005-2007] (veh/day)	Minimum	7,000	10,100
		Maximum	55,500	61,000
		Mean	24,200	22,809
		Std. dev	9,243	9,526
	Average AADT [2010-2012] (veh per day)	Minimum	5,625	10,000
		Maximum	58,750	56,800
		Mean	23,154	21,587
		Std. dev	9,463	8,693
	Number of Lanes	Minimum	2	2
		Maximum	8	6
		Mean	3.6	3.2
		Std. dev	1.1	1.2
	Right-Turn-on-Red (proportion of intersections)	Prohibited Limited	9%	8.50%
		Allowed	18%	20.50%
		Not-controlled	73%	71.00%
	Left Turn Lane	Not Present	8%	15%
	(proportion of intersections)	Present	92%	85%
	Posted Speed Limit (miles per hr)	Minimum	20	30
		Maximum	35	35
		Mean	29.9	30.5
		Std. dev	2.1	1.5
	Median	Not Present	67%	71%
		Present	33%	29%
Minor	Average AADT [2005-2007] (veh per day)	Minimum	375	4,800
		Maximum	40,150	27,500
		Mean	17,022	14,070
		Std. dev	5,989	4,872
	Average AADT [2010-2012] (veh per day)	Minimum	356	2,775
		Maximum	38,300	25,200
		Mean	16,136	13,333
		Std. dev	6,260	4,988
	Number of Lanes	Minimum	2	2
		Maximum	6	4
		Mean	2.6	2.7
		Std. dev	1	1
	Right-Turn-on-Red (proportion of intersections)	Prohibited	10%	12%
		Limited Allowed	19%	19%
		Not-controlled	71%	69%
	Left Turn Lane (proportion of intersections)	Not Present	13%	15%
		Present	87%	85%
	Median	Not Present	90%	96%
		Present	10%	4%

Model and Discussion

Using the method discussed above, a model fitting the annual number of injury crashes to the covariates can be estimated. The dataset was constructed as panel data containing the annual injury crash frequency in two time periods (2005-2007 and 2010-2012), while annual injury crash frequency, the presence of the RLC at intersections and some intersections characteristics changes over time. The dataset is split into two sets for modeling purposes, test and training sets. The test and training sets were sampled randomly, where the test and training datasets contained 20% and 80% of the intersections, respectively. The model was initially estimated using the training set, and the test set was used to evaluate the model performance. A binary variable was used to indicate the presence of an RLC at signalized intersections.

Table 3 summarizes the modeling results. The term α represents the decay rate of the exponential correlation function. According to the value of the exponential correlation function parameter (α), the spatial dependency between intersections dissipates within 3 kilometers (approximated with equation 5). As expected, the coefficient of intersections traffic is positive which implies that the more vehicles pass through the intersection, the more crashes will occur, although at a decreasing rate. A 1% increase in traffic in each lane is associated with a 0.5% increase in the probability of a crash. The results show that the more lanes that are linked to the intersection, the higher the probability of a crash. According to the model, the presence of a median in the minor approach improves the intersection safety by 8%. The effectiveness of RLC is shown by capturing a 6% lesser chance of crash for intersections equipped with a camera. Not only RLCs improve intersection safety but also reduces the probability of a crash by 2% within a 1 km radius. The land-use characteristics which have been examined in the form of the alcohol-serving POI density in 500, 700 and 1000 meters buffer, are correlated with the intersection ADT. Consequently, the variables with a dominant effect on crashes (intersection ADT) was used.

Table 3. Modeling results

	Variables	Estimate
Covariance Function Parameters	$\boldsymbol{\sigma^2}$	0.88
	$\boldsymbol{\alpha}$	0.53
Process Model Mean (μ)	Variables	Posterior Mean (Posterior Standard Deviation)
	Intercept	-3.12*** (0.77)
	Log of the average daily traffic in each lane	0.51 * (0.14)
	Number of lanes linked the intersection	0.02 * (0.00)
	Median presence in minor approach	-0.08 *** (0.03)
	RLC presence	-0.06 ** (0.02)
	Inverse distance of RLC to intersection (1/km)	-0.02 ** (0.00)
Goodness-of-Fit	MAD	3.15
	MPSE	25.41
	DIC	1107.61

- Asterisks *, **, and *** correspond with statistical significance levels at 5%, 10%, and 15%, respectively.
- Standard deviations in parenthesis.

Locating RLCs

The modeling results discussed above illuminate RLC impacts on injury crash frequencies at an intersection. To select the most efficient locations for installing RLCs, we specify an optimization problem with an objective function that seeks to maximize the impacts of RLC. Optimization ensures the maximum

reduction in injury crashes at intersections in the system after installing RLCs. The optimum solution is compared with the Chicago RLC system state in 2010. Crash data from the time period 2005-2007 used for evaluating the optimum solution. The objective function is defined as:

$$max \ \sum_{i=1}^{n}(c_C y_i l_i + \sum_{j=1}^{n} c_S y_i l_j d_{i,j}^{-1}) \quad (12)$$

subject to:

$$l_i = \begin{cases} 1 & if\ camera\ located\ at\ i \\ 0 & otherwise \end{cases} \quad (13)$$

$$l_j = \begin{cases} 1 & if\ camera\ located\ at\ j \\ 0 & otherwise \end{cases} \quad (14)$$

$$\sum_{i=1}^{n} l_i = R \qquad \forall i \in I \quad (15)$$

$$\sum_{j=1}^{n} l_j = R \qquad \forall j \in J \quad (16)$$

where l_i and l_j indicate if a camera is located at intersection i and j. The magnitude of the safety impact of camera presence at intersections is shown by c_C and the spillover effect is c_S . y_i and y_i represent the injury crash frequency at the intersection i and j, respectively. R is the total number of cameras in the system. For comparison purposes, the total number of cameras are constrained to 90 (number of cameras in 2010).

The optimized solution yielded to reduce the total number of injury crashes at intersections. The estimated optimum RLC locations are depicted in Figure 3. The total number of crashes in the system reduces by 13% after relocating the camera. In other words, camera allocation based on the model results can improve the system efficiency by 13%.

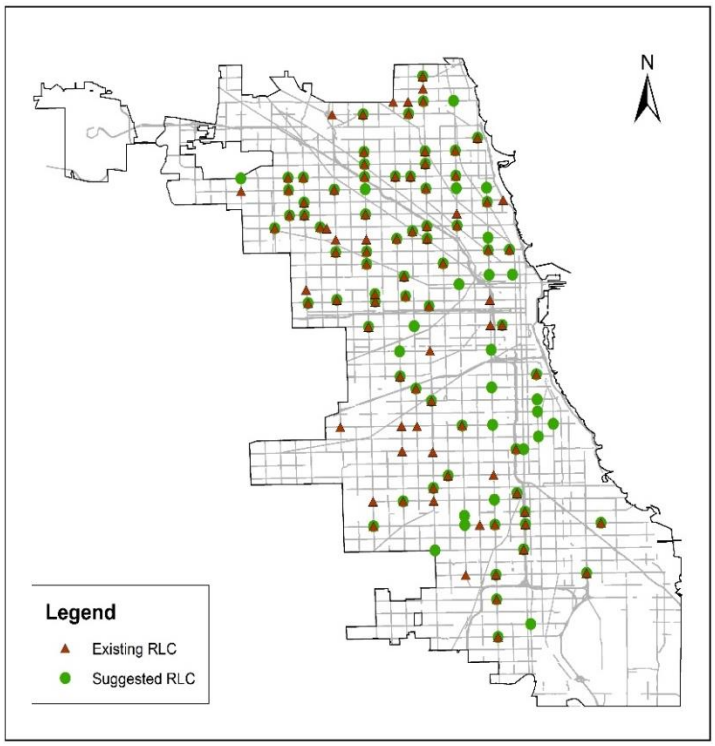

Figure 3. Suggested RLC locations across Chicago intersections

CONCLUSIONS

In this paper, a Bayesian hierarchical spatial model was developed for evaluating the RLC effect on injury crashes. The proposed model provides the capability of encountering unobserved heterogeneity in crashes and spatial dependency between intersections as well as capturing the spillover effect of RLC in the network. The model was developed using data collected at Chicago intersections. Among the various land-use and intersection characteristics, the crash frequency was associated with the traffic passing through the intersection, the size of the intersection in terms of the number of approach lanes, the presence of a divided median on the minor approach and the red-light enforcement at the intersection. The results shed further lights on the improving impact of RLCs on intersection safety by reducing the chance of an injury crash by 6% (all collision types). In addition, 2% fewer crashes are expected at intersections within 1 km network distance to the RLC location. From a practical standpoint, using the proposed model for analyzing the RLC performance can result in a reliable assessment of the program. Also, the results of this study can help previous attempts to investigate the economic feasibility of RLC programs and the allocation of RLCs in the network to achieve the highest efficiency [7, 32]. We defined an optimization problem using the captured RLC impacts, including the spillover effect, with the aim of maximizing the efficiency of RLCs in Chicago. Results show that the system performance can be improved by 13% after optimal camera allocation. More than 25% of the cameras need to be relocated to ensure maximum efficiency.

REFERENCES

1. Retting, R.A., et al., *Classifying urban crashes for countermeasure development.* Accident Analysis & Prevention, 1995. **27**(3): p. 283-294.
2. IIHS. 2017; Available from: http://www.iihs.org/iihs/topics/t/red-light-running/qanda#cite-text-0-0.
3. Hu, W. and J.B. Cicchino, *Effects of turning on and off red light cameras on fatal crashes in large US cities.* Journal of Safety Research, 2017. **61**: p. 141-148.
4. Council, F.M., et al., *Safety evaluation of red-light cameras*. 2005, United States. Federal Highway Administration. Office of Research and ….
5. Lord, D. and S. Geedipally, *Safety Effects of the Red-Light Camera Enforcement Program in Chicago, Illinois*. 2014, Lord Consulting, College Station, Texas.
6. Hill, S. and J. Lindly, *Red light running prediction and analysis*. 2003, University Transportation Center for Alabama.
7. Bonneson, J.A. and K. Zimmerman, *Development of guidelines for identifying and treating locations with a red-light-running problem*. 2004, Texas Transportation Institute, Texas A&M University System, College Station, Texas.
8. Elfar, A., et al. *Determinants of Red-light Camera Violation Behavior: Evidence from Chicago, Illinois*. in *TRB 2017 Annual Meeting*. 2017.
9. Lum, K. and Y. Wong, *Impacts of red light camera on violation characteristics.* Journal of Transportation Engineering, 2003. **129**(6): p. 648-656.
10. Yang, C. and W.G. Najm, *Analysis of red light violation data collected from intersections equipped with red light photo enforcement cameras*. 2006, National Highway Traffic Safety Administration.
11. F. Llau, A., et al., *The impact of red light cameras on crashes Within Miami–Dade County, Florida.* Traffic Injury Prevention, 2015. **16**(8): p. 773-780.
12. Washington, S. and K. Shin, *The impact of red light cameras (automated enforcement) on safety in Arizona*. 2005, Arizona Department of Transportation Chandler, AZ.
13. Miller, J., R. Khandelwal, and N. Garber, *Safety impacts of photo-red enforcement at suburban signalized intersections: an Empirical Bayes approach.* Transportation Research Record: Journal of the Transportation Research Board, 2006(1969): p. 27-34.
14. Pulugurtha, S.S. and R. Otturu, *Effectiveness of red light running camera enforcement program in reducing crashes: Evaluation using "before the installation","after the installation", and "after the termination" data.* Accident Analysis and Prevention, 2014. **64**: p. 9-17.
15. Retting, R. and M. Greene, *Influence of traffic signal timing on red-light running and potential vehicle conflicts at urban intersections.* Transportation Research Record: Journal of the Transportation Research Board, 1997(1595): p. 1-7.
16. Retting, R.A., S.A. Ferguson, and C.M. Farmer, *Reducing red light running through longer yellow signal timing and red light camera enforcement: results of a field investigation.* Accident Analysis & Prevention, 2008. **40**(1): p. 327-333.
17. Lord, D., F.J.T.r.p.A.p. Mannering, and practice, *The statistical analysis of crash-frequency data: a review and assessment of methodological alternatives.* Transportation Research Part A: Policy and Practice, 2010. **44**(5): p. 291-305.

18. Mannering, F.L. and C.R. Bhat, *Analytic methods in accident research: Methodological frontier and future directions.* Analytic Methods in Accident Research, 2014. **1**: p. 1-22.

19. Xu, P. and H. Huang, *Modeling crash spatial heterogeneity: random parameter versus geographically weighting.* Accident Analysis & Prevention, 2015. **75**: p. 16-25.

20. Huang, H., et al., *A multivariate spatial model of crash frequency by transportation modes for urban intersections.* Analytic Methods in Accident Research, 2017. **14**: p. 10-21.

21. Cheng, W., et al., *Multimodal crash frequency modeling: Multivariate space-time models with alternate spatiotemporal interactions.* Accident Analysis & Prevention, 2018. **113**: p. 159-170.

22. Alarifi, S.A., M. Abdel-Aty, and J. Lee, *A Bayesian multivariate hierarchical spatial joint model for predicting crash counts by crash type at intersections and segments along corridors.* Accident Analysis and Prevention, 2018. **119**: p. 263-273.

23. Guo, F., X. Wang, and M.A. Abdel-Aty, *Modeling signalized intersection safety with corridor-level spatial correlations.* Accident Analysis & Prevention, 2010. **42**(1): p. 84-92.

24. Hobeika, A. and N. Yaungyai, *Evaluation update of the red light camera program in Fairfax County, VA.* IEEE Transactions on Intelligent Transportation systems, 2006. **7**(4): p. 588-596.

25. Shin, K. and S. Washington, *The impact of red light cameras on safety in Arizona.* Accident Analysis and Prevention, 2007. **39**(6): p. 1212-1221.

26. Høye, A., *Still red light for red light cameras? An update.* Accident Analysis & Prevention, 2013. **55**: p. 77-89.

27. Ahmed, M.M. and M. Abdel-Aty, *Evaluation and spatial analysis of automated red-light running enforcement cameras.* Transportation Research Part C: Emerging Technologies, 2015. **50**: p. 130-140.

28. Banerjee, S., B.P. Carlin, and A.E. Gelfand, *Hierarchical modeling and analysis for spatial data*. 2014: CRC press.

29. Mahmassani, H.S., et al., *Chicago Red Light Camera Enforcement: Best Practices and Program Road Map*. 2017, Northwestern University Transportation Center, Evanstone, Illinois.

30. Summala, H. and T. Mikkola, *Fatal accidents among car and truck drivers: effects of fatigue, age, and alcohol consumption.* Human Factors, 1994. **36**(2): p. 315-326.

31. Jonah, B.A., *Sensation seeking and risky driving: a review and synthesis of the literature.* Accident Analysis & Prevention, 1997. **29**(5): p. 651-665.

32. Claros, B., C. Sun, and P. Edara, *Safety effectiveness and crash cost benefit of red light cameras in Missouri.* Traffic injury prevention, 2017. **18**(1): p. 70-76.